Original Article

Dose Estimation Using Optically Stimulated Luminescence Dosimeter and EBT3 Films for Various Treatment Techniques in Alderson Rando Phantom and Estimation of Secondary Cancer Incidence for Carcinoma of Left Breast

N. Sushma[1,2], Shanmukhappa Kaginelli[2], P. Sathiyaraj[1], Sakthivel Vasanthan[3], K. M. Ganesh[1]

[1]Department of Radiation Physics, Kidwai Memorial Institute of Oncology, Bengaluru, [2]Division of Medical Physics, JSS Academy of Higher Education and Research, Mysuru, Karnataka, India, [3]Advanced Medical Physics, Houston, Texas, USA

Abstract

Aim: The aim of this study was to measure the dose to planning target and organ at risk (OAR) using Alderson Rando phantom for various treatment techniques in left breast radiotherapy and to estimate the secondary cancer incidence. **Materials and Methods:** Eleven different combinations of plans containing four techniques (three dimensional conformal radiotherapy, intensity-modulated radiation therapy [IMRT], volumetric modulated arc therapy [VMAT], and combination of 3DCRT and VMAT plans (HYBRID)) were created with 6 MV FF and 6 MV FFF (flattening filter and flattening filter-free) photon energies in phantom. Planned target volume and OAR doses in 23 different locations were measured using optically stimulated luminescence dosimeter (OSLD) and EBT3 films. Assuming the age of exposure as 30 years, lifetime attributable risk (LAR) was estimated based on excess absolute risk (EAR) models outlined in the Biological Effects of Ionizing Radiation VII report. **Results:** Film showed maximum deviations of 6.15% with IMRT_C_FF plan when compared with treatment planning system (TPS). The maximum percentage difference of 1.7% was found with OSLD measurement when compared with TPS for VMAT_T_FFF plan. EAR estimation was done for all the OARs including target. The LARs for left lung, right lung, and right breast were evaluated. The maximum LAR values of 2.92 ± 0.14 were found for left lung with VMAT_C_FFF plans. **Conclusion:** This study shows that both OSLD and EBT3 films are suitable for dose measurements using Rando phantom. OSLD shows superior results when compared with films, especially with relatively larger distances. Maximum LAR values were found with VMAT_C_FFF plans. Considering the secondary cancer risk associated with the patients treated in the younger age group, it is suggested that *in vivo* dose estimation should be a part of treatment quality audit whenever possible.

Keywords: Gafchromic EBT3 films, lifetime attributable risk, optically stimulated luminescence dosimeter

Received on: 12-05-2022 **Review completed on: 29-08-2022** **Accepted on: 30-08-2022** **Published on: 08-11-2022**

Introduction

Breast cancer is a common and prevalent cancer in women. During radiotherapy treatment with high-energy photon beams, a small fraction of the delivered dose is absorbed a few centimeters away from the irradiated field.[1] The dose distributions are usually verified inside the planned target volume (PTV) only. Low-dose radiation received by the organs falling out of the treatment field might have long-term effects such as development of subsequent malignancies, and hence the estimation of out-of-field dose is necessary to evaluate late complications. Two large cohort studies reported that second cancers occurring after radiation therapy for breast cancer are found mostly in organs adjacent to the previously treated fields, such as the organs exposed to the highest radiation dose.[2,3] Concerns have been raised about the potential increase of radiation-induced secondary cancer risk associated with these new technologies, mainly in the contralateral breast and lungs.[4,5]

Access this article online

Quick Response Code:

Website: www.jmp.org.in

DOI: 10.4103/jmp.jmp_36_22

Address for correspondence: Dr. K. M. Ganesh, Department of Radiation Physics, Kidwai Memorial Institute of Oncology, Dr. M.H. Marigowda Road, Bengaluru - 560 029, Karnataka, India. E-mail: kmganesh1@gmail.com

How to cite this article: Sushma N, Kaginelli S, Sathiyaraj P, Vasanthan S, Ganesh KM. Dose estimation using optically stimulated luminescence dosimeter and EBT3 films for various treatment techniques in Alderson Rando phantom and estimation of secondary cancer incidence for carcinoma of left breast. J Med Phys 2022;47:225-34.

In vivo dosimetry for radiotherapy patients is required to ensure that the dosage delivered to the patient conforms to the prescribed dose as predicted by the treatment planning system (TPS).[6] *In vivo* dosimetry is recognized as part of the quality assurance program in radiotherapy. Various types of detectors are used to measure *in vivo* doses such as diamond detectors, thermoluminescence dosimeters (TLDs), and ion chamber using water phantom or anthropomorphic phantom.[7-9] Measurements were made by cylindrical ion chamber at distances of 10–30 cm from the field edges. Out-of-field contributions of radiation dose for intensity-modulated radiation therapy (IMRT) and volumetric modulated arc therapy (VMAT) were measured using Gafchromic films and compared with calculations using a superposition/convolution-based TPS.[10] Comparison of second cancer risk due to out-of-field doses from 6-MV IMRT and proton therapy based on six pediatric patient treatment plans was reported in the literature.[11] Optically stimulated luminescence (OSL) has been brought into radiation dosimetry, and the use of an OSL dosimeter (OSLD) for dose verification in clinical radiotherapy is gaining popularity.[12-14] OSLD exhibits high accuracy and precision in dose determination, reusability, multiple readout, and readability even after a long postirradiation time lapse.[15] Despite the capability to measure small and large doses, the drawback is that the phosphor material (Al2O3:C) is sensitive to light owing to the nature of OSL phenomenon. However, this drawback is easily overcome by a water-equivalent light-tight plastic encapsulation.

One of the significant late effects of radiation therapy is radiation-induced secondary cancers. The absolute risk of subsequent cancer caused by stray treatment radiation was determined to be 1.4% for patients who survived more than 10 years after treatment.[16] It has a significant impact on ideal treatment decision-making. Many factors contribute to the development of second cancer such as age at radiation, dose and volume of irradiated area, type of irradiated organ and tissue, and radiation technique. Exact contrivance of second cancer is unknown. Even if radiation-induced cancers are rare, they must be kept in mind each time a radiotherapy is proposed.

We intended to assess the incidence of cancer based on measured dose data rather than TPS-based calculations because the computation of out-of-field dose by TPS always deviates considerably (up to 40%) from the actual dose.[17,18] Thus, in this study, an attempt was made to customize the Anthropomorphic Rando phantom to measure the doses in target and organs at risk (OARs) using nanoDot OSLD and Gafchromic EBT3 film in left breast irradiation. The assessments were made by comparing point doses in 24 different locations in the PTV and OARs both put together. As the incidences of secondary cancer are increasing in breast cancer patients due to increased survival rates, it is essential to estimate the secondary cancer risk in women for the OARs associated with the treatment of carcinoma of left breast. Hence, the secondary risk estimation was calculated with lifetime attributable risk (LAR) and excess absolute risk (EAR) formalism using the Biological Effects of Ionizing Radiation (BEIR) VII[19] concept assuming the age of exposure as 30 years.

Materials and Methods

In this study, Elekta Versa HD™ linear accelerator with 6 MV FF and FFF beams was used with a beam quality index of 0.676 and 0.668, respectively. The linear accelerator is equipped with Agility™ multileaf collimators having 80 pairs of leaves of width 5 mm each.

Phantom, treatment planning, and dosimeters

The Alderson Rando phantom designed to use for dose measurement with TLD was customized to accommodate the OSLD and EBT3 films. Currently existing 5 mm holes suitable to insert TLD rods were modified by matching a groove of 2 mm slots on either side with 1.2 cm × 1.7 cm deep centered over the existing holes to allow the placement of OSLD s and EBT3 films. The Alderson Rando phantom images were taken using Philips Big Bore Brilliance computed tomography (CT) scanner with 3-mm slice thickness and exported to the TPS for delineation of the target and OAR. PTV was delineated for whole left breast based on Radiation Therapy Oncology Group breast cancer atlas. All OARs and target were delineated by an experienced radiation oncologist. Thirteen OARs such as contralateral breast, right and left lenses, right and left lobe of thyroid, right and left lung, right and left kidney, spinal cord, heart, liver, bladder, rectum, and uterine were contoured on Digital Imaging and Communications in Medicine (DICOM) images. The OARs and target within the close proximity to the radiation field consisted of 3 measurement locations (PTV_1, PTV_2, PTV_3 represents the three locations of dosimeter placements inside the PTV volume. Lt Lung_1,2,3: represents the three locations of dosimeter placements inside the left lung. Rt Lung_1,2,3 represents the three locations of dosimeter placements inside the Right Lung. Rt Breast_1,2,3represents the three locations of dosimeter placements inside the right Breast), respectively. Treatment planning was done using Monaco TPS (version 5.11.03) with Monte Carlo and collapsed cone algorithms for IMRT, VMAT, and three dimensional conformal radiotherapy (3DCRT), respectively, on Rando phantom's DICOM images. To evaluate and compare the point dose of PTV and out-of-field organs in breast cancer, 11 different plans containing four techniques (3DCRT, IMRT, VMAT, and HYBRID) were created. 3DCRT plans were generated with 2 tangential opposed fields; conventional IMRT plans were generated with 5 fields equally spaced angles; tangential IMRT plans were generated with 4 fields arranged in tangential beam angles; hybrid plans were generated with 70%–30% and 80%–20% dose contribution from 3DCRT and VMAT, respectively. Dose prescription was 5000 cGy in 25 fractions to PTV in treatment plans generated using 6FF and 6FFF energies by different treatment techniques. The generated treatment plans were 3DCRT_FF, IMRT Conventional using FF and FFF beams (IMRT_C_FF and IMRT_C_FFF), IMRT Tangential using FF and FFF beams (IMRT_T_FF and IMRT_T_FFF), VMAT Conventional

using FF and FFF beams(VMAT_C_FF and VMAT_C_FFF), VMAT Tangential using FF and FFF beams(VMAT_T_FF and VMAT_T_FFF), Hybrid plans were generated with 70%–30% and 80%–20% dose contribution from 3DCRT and VMAT, respectively, HYBRID 70/30 (HYB_70/30) and HYBRID 80/20 (HYB_80/20). All the plans were optimized to cover PTV to clinically acceptable level (95% of the prescribed dose to cover 95% of PTV) and spare the OARs to acceptable tolerance limit. Figure 1 illustrates few Rando phantom slices with OSLD positions. Figure 2 illustrates a typical HYBRID 70/30 plan in Monaco TPS.

Two types of dosimeters were used to find the point dose of 24 locations in Rando phantom: first, the nanoDot OSLDs (Landauer, Inc., Glenwood, USA) and the next one being the Gafchromic EBT3 films. NanoDot OSLDs (OSLD) consist of plastic discs of Al2O3:C of 5 mm diameter and 0.2 mm thickness. It was encased in 1 cm × 1 cm × 0.2 cm light-tight black plastic case with a mass density of 1.03 g/cm^3, to prevent the signal depletion due to light. The sensitive element in the disc can slide out of the plastic case during read-out process and optical bleaching. The bar code provided in each OSLD enables to identify, to track the history, and to record with ease. The OSLD system used is shown in Figure 3.

The Gafchromic EBT3 films of size 13" ×17" were carefully cut into 1 cm × 1 cm to find the point dose in this study. EBT3 films have a single active layer with 28 µm thick and contain the active component, a marker dye. The active layer is between two 125 µm transparent matte polyester subtracts. After irradiation, the films were digitized and the pixel value was converted to dose using the obtained calibration curve.

Calibration of detectors

NanoDot optically stimulated luminescence dosimeter

Element correction factor (ECF) was determined as the ratio of the response of each OSLD to the average response of 100 OSLDs as a multiplicative factor. To determine the ECF, a teletherapy Cobalt-60 beam with a uniform dose profile was used to irradiate 100 OSLDs simultaneously to a known dose of 200 cGy with a field size of 20 cm × 20 cm at 5 cm depth. The ECF for each OSLD was determined from the batch irradiated with 100 OSLDs. The corrected OSLD dose (D_{corr})

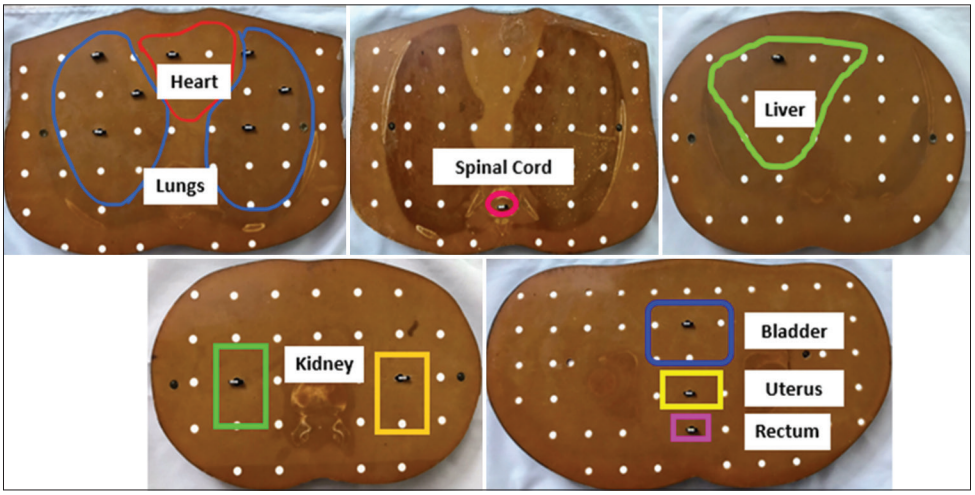

Figure 1: Pictures showing the OSLD placement in various organs in Rando phantom. OSLD: Optically stimulated luminescence dosimeter

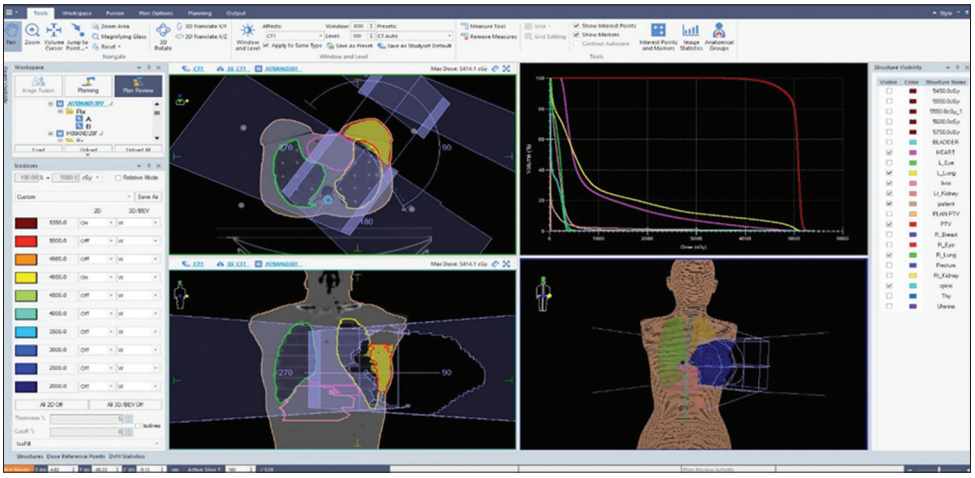

Figure 2: Illustration of HYBRID 70/30 plan with 95% isodose (in yellow color) from tangential beams and a partial arc in treatment planning system

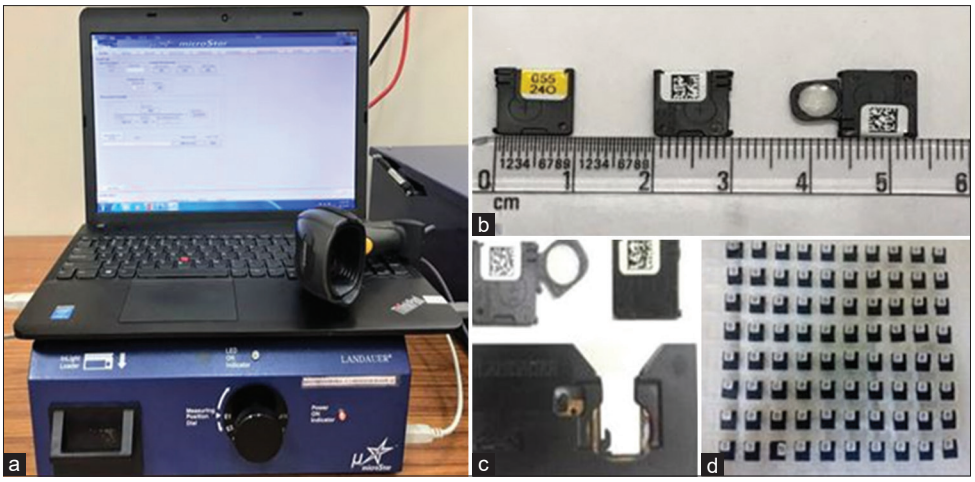

Figure 3: Picture of OSLD dosimetry system: (a) MicroStar reader with external PC and bar coder, (b) NanoDot OSL dosimeter with unique ID number and backside showing unique barcode, (c) NanoDot OSLD adapter, (d) OSLD arranged in rows in slab phantom for calibration. OSL: Optically stimulated luminescence, OSLD: OSL dosimeter

was calculated using the following equation:

$$R_{corr} = ECF \times D \quad \text{(Eq. 1)}$$

$$D = (D_a - D_b) \quad \text{(Eq. 2)}$$

Where D_b and D_a are the doses of the OSLD before and after irradiation. The ECF obtained was applied to raw readings in the subsequent uses of each dosimeter in all measurements. OSLDs were exposed to a dose ranging from 25 cGy to 1000 cGy and were normalized to 200 cGy.

Gafchromic (EBT3) films

The calibration of EBT3 films was done by irradiating the films at 5 cm depth in solid water-equivalent phantom. The films were irradiated with 6 MV photon beam with a source-to-surface distance of 95 cm. Films of size 4 cm × 4 cm were exposed to the doses of 10, 20, 30, 40, 50, 100, 150, 200, 250, 300, 350, 400, 450, 500, 600, and 700 cGy with a field size of 10 cm × 10 cm, and the nonirradiated film (0 Gy) was taken as reference. All films were scanned 24 h after irradiation using Epson 12000XL (Epson America, Inc., Long Beach, USA) flatbed document scanner. The films were analyzed using PTW Mephysto 3.0 software which includes film scanning (FilmScan), calibration (FilmCal), and film analyzing (FilmAnalyse) modules. The mean pixel value was obtained from central region of 1 cm × 1 cm. The net optical density (OD) was expressed against control film as a logarithmic value of ratio of mean pixel value unexposed versus exposed film. All measurements of the film were performed twice to verify the reproducibility of the results.

Estimation of secondary cancer risk

EAR, excess relative risk (ERR), and LAR were calculated using the BEIR VII model. ERR was defined as an excess risk with respect to background risk, and EAR as the difference between total and background risk. The equation for EAR and LAR is:

$$EAR\,(D,s,e,a) = \beta D ex[\,(\gamma\,[e-25]/10)\,(a/50)^{\eta}$$
$$where\ \beta = 9.9;\ \gamma = -0.51;\ \eta = 3.5\ for\ a < 50$$
$$and\ 1.1\ for\ a \geq 50 \quad \text{(Eq.3)}$$

where D = dose; β, γ, and η are ERR- and EAR-specific parameters for various organs for each sex; e is age at exposure; a is attained age.

$$LAR = \int_{age_{x+L}}^{age_{a,0}} EAR(D, age_x, age_a)\,\frac{S(age_a)}{S(age_x)}\,d(age_a) \quad \text{(Eq.4)}$$

The integration over EAR was performed over an attained age from a latent period (L) of solid cancer induction after the exposure to age$_a$ of 70 years. The ratio S (age$_a$)/S (age$_x$) defines the probability of surviving from age at exposure to the attained age.

Age is one of the key parameters impacting the risk of radio-induced secondary malignancies. Several risk models have been developed to estimate cancer incidence and mortality. The uncertainties associated with each of the models are close to, or exceed, the variation between the models. We have chosen to use the BEIR VII model as it provides model parameters for specific organs for each sex and includes a parameter describing incidence with age at exposure and attained age. Our focus was to estimate cancer incidence over an age range of 35–80 years. For breast cancer, the BEIR VII Committee used only an EAR model to quantify risk. The model was based on a pooled analysis of eight cohorts. Although there was no simple EAR model that adequately describes the excess risks in all cohorts, the BEIR VII EAR model provides a reasonable fit to data from four of the cohorts. In the BEIR VII model, the EAR depends on both age at exposure and attained age. Unlike for other cancers, the EAR continues to decrease exponentially with age at exposure throughout one's lifetime, and the EAR increases with attained age less rapidly after age 50. We have evaluated LAR via the method given in the BEIR VII report.

Because the population standard deviation and the mean value of a sample selected from a normally distributed population are unknown. To check the significance of our results, Student's *t*-test was used for statistical analysis and the *P* value was set to 0.05 ($P \leq 0.05$). The precision of the measurements is expressed as standard deviation from repeated measurements. The accuracy of the measurements is expressed as percentage difference with respect to TPS values.

Results

Optically stimulated luminescence dosimeter and film calibration

The spread in ECF values ranged between 0.978 and 1.01. Figure 4 presents the dose–response behavior of nanoDot OSLDs with Co-60 and 6 MV photon beams. The OSLD response was linear for doses from 25 to 300 cGy, and a supralinear dose response was observed above 300 cGy. The reproducibility of OSLD was investigated by exposing OSLDs to identical doses of 2, 4, 6, 8, and 10 Gy three times each. The inter-OSL response variation was found with maximum of 0.9% for dose level up to 10 Gy with 6 MV photon beams, which indicated a good reproducibility of OSLD during multiple irradiations.

A third-degree polynomial function was used to fit the calibration curve of the film with radiation dose against net OD, as shown in Figure 5.

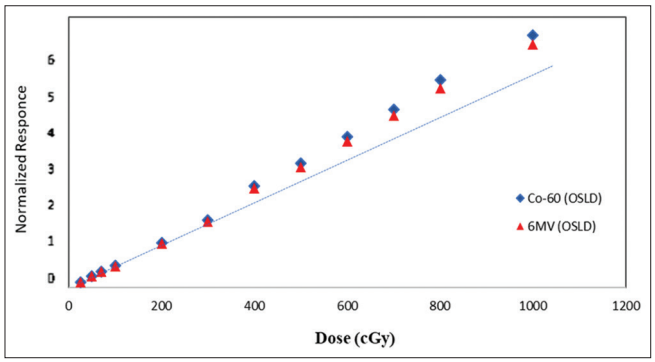

Figure 4: Dose–response curve of nanoDot OSLD for photon beam. OSLD: Optically stimulated luminescence dosimeter

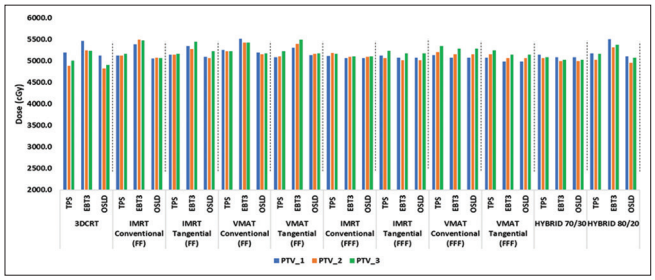

Figure 6: Comparison of TPS-calculated target dose with the OSLD- and EBT3-measured doses. OSLD: Optically stimulated luminescence dosimeter, TPS: Treatment planning system

Target dose

Figure 6 represents the comparison of TPS-calculated target dose (PTV_1, PTV_2, and PTV_3) with the OSLD- and EBT3-measured data with different treatment planning techniques. It was observed that film shows maximum deviations than OSLD irrespective of planning modalities; in the film measurement, the maximum deviation was found as 6.15% with TPS-calculated dose for IMRT_C plan. OSLDs show less deviations than film irrespective of planning modalities. A maximum difference of 1.7% was noticed in VMAT_T_FFF plan when compared to TPS-calculated dose. In all plans except for VMAT_T, the measured dose with OSLDs was less than the TPS-calculated dose. The average percentage difference of measured dose with film and OSLDs was 4.9%±0.79 and 1.1%±0.54, respectively.

Organ at risk

Figure 7 shows the percentage difference between OSLD and film with respect to TPS-calculated doses. The OAR doses measured with OSLDs were well in agreement with TPS-calculated doses with a maximum percentage difference of 2.3% for the right kidney. For film, the percentage difference between measured and calculated doses was high with a maximum deviation of 10.7% for left lung. Films were not able to measure few OAR doses which were far away from the target [Figure 8].

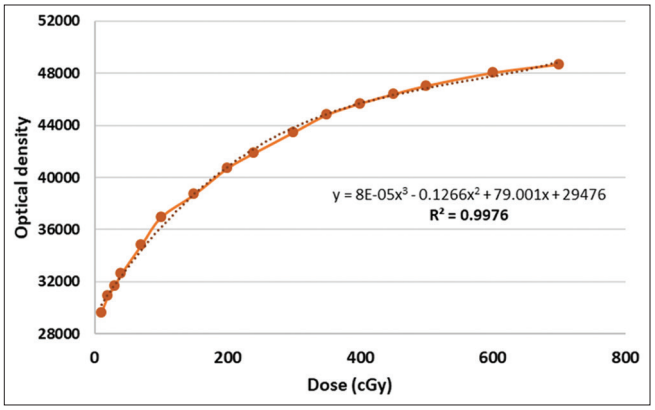

Figure 5: The dose calibration curve for EBT3 film

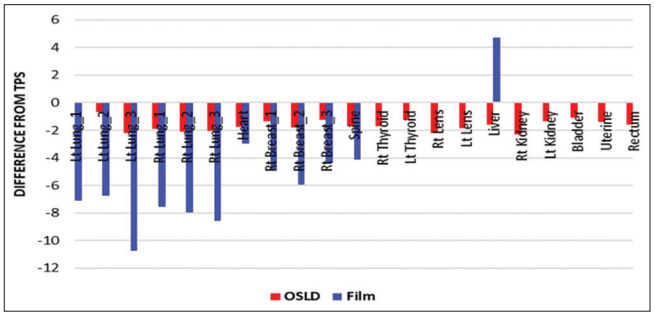

Figure 7: Percentage difference of measured OAR doses of OSLD and film with respect to TPS. OSLD: Optically stimulated luminescence dosimeter, TPS: Treatment planning system

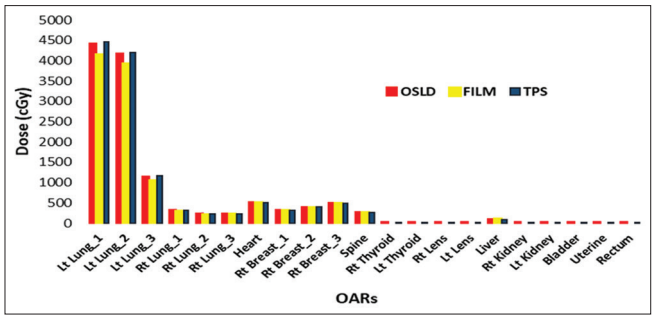

Figure 8: OAR doses calculated from TPS and dose measured with OSLD and films. OSLD: Optically stimulated luminescence dosimeter, TPS: Treatment planning system

Table 1 represents the peripheral dose measured in thorax region (organs closer to PTV). The dose measured with OSLDs was higher than the films for the OARs in the thorax region. As the distance increases between the OARs and the plan isocenter, the reduction in dose was evident. The maximum dose in left lung was found in IMRT_C_FF and IMRT_T_FF techniques with doses of 37.2 Gy, 32.8 Gy and 36.9 Gy, 34.8 Gy for OSLD and films, respectively. Similarly, the maximum dose in right lung is found in VMAT_C_FF and IMRT_T_FFF techniques and doses were 3.85 Gy, 3.5 Gy and 3.7 Gy, 3.2 Gy, respectively. Similar results for heart and right breast were found with IMRT_T_FF and IMRT_T_FFF techniques. As far as spine was concerned, it was found that VMAT_C_FF and VMAT_C_FFF treatment techniques had maximum doses with both OSLD and films.

Secondary cancer risks

Table 2 shows the mean dose per organ calculated from both OSLD and films with all radiotherapy plans. The pattern in the dose data was expected. Distant organs received mean doses less than 0.3 Gy with higher doses close to the target. The two complex techniques such as HYB_80/20 and HYB_70/30 delivered higher doses to most of the OARs than the standard tangential plans. A significant difference was seen between the said techniques with the mean contralateral lung and contralateral breast doses.

Excess absolute risk

Based on the data from all the delivered techniques, EAR values for age at exposure of 30 years to the attained age of 45 and 60 years are presented in Tables 3 and 4.

Lifetime attributable risk

The LAR values are dominated by the radiotherapy contribution to total dose. The LAR values are lowest for lens, thyroid, liver, and bladder, and there is little impact from radiotherapy technique observed in the data for these organs. LARs were calculated for lungs and right breast. LARs of left lung ranged between 1.73 ± 2.01 (per 100 persons) and 2.82 ± 1.09 with 3DCRT and VMAT_C_FF techniques, respectively. The values for right lung were seen between 0.91 ± 0.23 and 2.05 ± 0.79 with IMRT_C_FF and VMAT_T_FF, respectively. The LARs for right breast were found between 0.33 ± 1.65 and 2.69 ± 1.75

Table 1: The measured values (dose±standard deviation) of peripheral dose (cGy) measured in thorax region

Technique	Left lung		Right lung		Heart		Right breast		Spine	
	OSLD	Film	OSLD	Film	OSLD	Film	OSLD	Film	OSLD	Film
3DCRT	3044.03±4.4	2902.78±37.5	60.24±0.3	63.88±17.5	204.88±1.7	200.0±20.4	94.03±1.0	94.44±22.0	49.63±0.4	50.0±0.0
IMRT_C_FF	3721.78±10.2	3288.89±47.3	191.67±1.5	186.11±21.1	543.87±7.1	500.0±20.4	326.32±0.7	313.89±31.5	211.18±0.2	191.67±11.8
IMRT_T_FF	3690.73±9.2	3483.33±24.9	289.76±4.8	269.44±15.7	801.44±8.9	750.0±20.4	569.88±4.8	541.67±24.7	258.78±0.8	241.67±23.6
VMAT_C_FF	3336.43±11.3	3144.44±28.6	385.20±3.9	355.56±15.7	509.48±2.7	466.67±11.8	507.75±7.7	463.89±18.3	373.51±9.1	350.0±20.4
VMAT_T_FF	3155.44±16.3	2980.56±24.7	228.45±1.6	216.67±30.1	383.08±2.3	358.33±23.6	432.52±4.9	394.45±25.1	216.25±1.8	216.26±1.8
IMRT_C_FFF	3552.43±20.5	3297.22±82.6	155.03±1.8	158.33±13.6	503.88±2.3	533.33±11.8	310.26±1.9	325.0±14.7	222.62±0.4	250.0±20.4
IMRT_T_FFF	3543.56±13.0	3313.89±27.6	373.29±1.9	327.78±17.5	933.65±3.6	1041.67±51.4	616.16±8.7	594.44±18.6	161.52±1.7	183.33±11.8
VMAT_C_FFF	3454.56±9.6	3308.33±21.1	330.74±2.5	302.78±17.5	464.01±2.4	425.0±20.4	389.0±1.8	361.11±19.6	489.33±2.1	450.0±20.4
VMAT_T_FFF	3289.28±9.9	3086.11±62.5	211.07±1.4	194.44±14.7	353.91±2.1	333.33±11.8	411.76±4.2	430.56±28.5	302.95±0.6	283.33±31.2
HYB 80/20	2242.69±3.3	2127.78±22.2	274.85±2.4	277.77±14.7	446.75±4.2	425.0±20.4	349.39±2.0	333.33±20.4	210.75±1.5	233.33±11.8
HYB 70/30	2576.61±6.5	2400.0±25.1	260.49±1.4	238.89±39.1	381.32±1.9	425.0±20.4	340.33±2.4	336.11±24.0	288.64±1.5	266.67±62.4

OSLD: Optically stimulated luminescence dosimeter, 3DCRT: 3D conformal radiotherapy, IMRT: Intensity-modulated radiation therapy, VMAT: Volumetric modulated arc therapy, HYB: Hybrid, FF: Flattening filter, FFF: FF free

Table 2: The mean dose (cGy) per organ calculated from both optically stimulated luminescence dosimeter and films from all the delivered plans

OARs	Plan										
	3DCRT	IMRT_C_FF	IMRT_T_FF	VMAT_C_FF	VMAT_T_FF	IMRT_C_FFF	IMRT_T_FFF	VMAT_C_FFF	VMAT_T_FFF	HYB 80/20	HYB 70/30
Left lung	0.6088	0.7444	0.7381	0.6673	0.6311	0.7105	0.7087	0.6909	0.6579	0.5153	0.4485
Right lung	0.012	0.0383	0.058	0.077	0.0457	0.031	0.0747	0.0661	0.0422	0.0521	0.055
Heart	0.041	0.1094	0.1611	0.1026	0.0778	0.1014	0.1891	0.0943	0.0712	0.0772	0.0899
Right breast	0.0188	0.0653	0.114	0.1016	0.0865	0.0621	0.1232	0.0778	0.0824	0.0681	0.0699
Spine	0.01	0.0425	0.0515	0.0757	0.0439	0.0448	0.0328	0.0985	0.061	0.0583	0.0428
Thyroid	0.0101	0.0028	0.0034	0.0033	0.0033	0.0029	0.0033	0.0032	0.0034	0.0062	0.0068
Lens	0.0029	0.0006	0.0006	0.0006	0.0006	0.0007	0.0007	0.0007	0.0007	0.0016	0.0017
Liver	0.0095	0.0183	0.0173	0.021	0.0195	0.0158	0.0148	0.0195	0.0206	0.0261	0.0208
Kidney	0.0035	0.0024	0.0028	0.0027	0.0021	0.0022	0.0025	0.0023	0.0018	0.003	0.003
Bladder	0.0014	0.0012	0.0018	0.0018	0.0006	0.0008	0.0014	0.001	0.0006	0.0043	0.0048
Uterus	0.0008	0.0018	0.0018	0.0012	0.0016	0.001	0.0014	0.0006	0.0012	0.0044	0.0047
Rectum	0.0026	0.0004	0.0012	0.0016	0.0008	0.0012	0.0016	0.0008	0.0008	0.0039	0.0039

OAR: Organ at risk, 3DCRT: 3D conformal radiotherapy, IMRT: Intensity-modulated radiation therapy, VMAT: Volumetric modulated arc therapy, HYB: Hybrid, FF: Flattening filter, FFF: FF free

Table 3: Excess absolute risk values for age at exposure of 30 years to the attained age of 45 years in various treatment techniques

OARs	Plan										
	3DCRT	IMRT_C_FF	IMRT_T_FF	VMAT_C_FF	VMAT_T_FF	IMRT_C_FFF	IMRT_T_FFF	VMAT_C_FFF	VMAT_T_FFF	HYB 80/20	HYB 70/30
Left lung	4.192	4.435	4.398	3.98	3.76	4.233	4.222	4.116	3.919	3.07	2.672
Right lung	0.718	2.284	3.453	4.59	2.722	1.847	4.448	3.941	2.515	3.104	3.275
Heart	0.224	0.599	0.882	0.56	0.426	0.555	1.035	0.516	0.389	0.422	0.492
Right breast	3.766	13.07	22.826	20.34	17.324	12.427	24.68	15.581	16.493	13.632	13.995
Spine	0.055	0.233	0.282	0.41	0.24	0.245	0.18	0.539	0.334	0.319	0.234
Thyroid	0.141	0.038	0.047	0.05	0.045	0.041	0.045	0.044	0.048	0.086	0.094
Lens	0.017	0.004	0.004	0	0.004	0.004	0.004	0.004	0.004	0.01	0.01
Liver	0.159	0.306	0.289	0.35	0.325	0.264	0.248	0.325	0.344	0.435	0.347
Kidney	0.058	0.039	0.046	0.04	0.034	0.036	0.041	0.039	0.031	0.05	0.05
Bladder	0.016	0.014	0.021	0.02	0.007	0.009	0.016	0.011	0.007	0.05	0.055
Uterus	0.009	0.021	0.021	0.01	0.018	0.012	0.016	0.007	0.014	0.05	0.055
Rectum	0.03	0.005	0.014	0.02	0.009	0.014	0.018	0.009	0.009	0.046	0.046

Values indicate the risk of getting secondary cancers per 100 irradiated patients when they attain 45 years of age. Calculation based on BEIR VII report. BEIR: Biological Effects of Ionizing Radiation, 3DCRT: 3D conformal radiotherapy, IMRT: Intensity-modulated radiation therapy, VMAT: Volumetric modulated arc therapy, HYB: Hybrid, FF: Flattening filter, FFF: FF free, OAR: Organ at risk

Table 4: The excess absolute risk values for age at exposure of 30 years to the attained age of 60 years in various treatment techniques

OARs	Plan									
	3DCRT	IMRT_C_FF	IMRT_T_FF	VMAT_C_FF	VMAT_T_FF	IMRT_C_FFF	IMRT_T_FFF	VMAT_C_FFF	VMAT_T_FFF	HYB 80/20	HYB 70/30
Left lung	5.292	5.635	5.798	5.997	5.500	5.433	5.325	5.091	4.979	4.097	4.867
Right lung	2.038	6.484	9.803	13.032	7.729	5.245	12.629	11.189	7.141	8.813	9.298
Heart	0.637	1.700	2.503	1.594	1.209	1.575	2.937	1.465	1.105	1.199	1.396
Right breast	7.602	16.382	26.074	21.051	24.969	15.084	29.816	21.450	23.290	17.516	18.248
Spine	0.156	0.660	0.799	1.176	0.681	0.696	0.510	1.530	0.948	0.905	0.665
Thyroid	0.400	0.109	0.134	0.131	0.129	0.115	0.128	0.125	0.135	0.244	0.268
Lens	0.049	0.011	0.011	0.011	0.011	0.012	0.013	0.012	0.012	0.028	0.029
Liver	0.362	0.696	0.657	0.797	0.740	0.600	0.564	0.739	0.783	0.991	0.790
Kidney	0.131	0.090	0.105	0.102	0.078	0.082	0.094	0.088	0.070	0.114	0.114
Bladder	0.053	0.046	0.070	0.070	0.023	0.031	0.054	0.038	0.023	0.168	0.184
Uterus	0.031	0.069	0.070	0.047	0.061	0.039	0.054	0.023	0.046	0.168	0.183
Rectum	0.100	0.015	0.046	0.063	0.031	0.047	0.061	0.030	0.030	0.152	0.152

Values indicate the risk of getting secondary cancers per 100 irradiated patients when they attain 60 years of age. Calculation based on BEIR VII report. BEIR: Biological Effects of Ionizing Radiation, 3DCRT: 3D conformal radiotherapy, IMRT: Intensity-modulated radiation therapy, VMAT: Volumetric modulated arc therapy, HYB: Hybrid, FF: Flattening filter, FFF: FF free, OAR: Organ at risk

for 3DCRT and VMAT_C_FFF techniques, respectively, as shown in Table 5.

Discussion

There is a need to analyze the doses to the OARs and their corresponding long-term risks in radiotherapy, particularly with advanced treatment techniques. In cases where the doses may be more critical with some of the OARs, it is worthwhile considering the various influences of such dose. Wherever possible, attempts should be made to choose delivery parameters that result in an uncompromised dose coverage to target with less dose to OARs.

For dose measurements in Rando phantom using OSLD and film, 11 different treatment plans were selected and measurements were carried out at 23 different locations for both target and OARs. The maximum dose measured by the OSLD and films was noticed with the OARs such as lung, heart, and contralateral breast which were close to the target. OSLDs could detect signals even when they were placed far from the target, whereas films which were placed far from target could not detect the dose due to its limitations. This difference of dose detection by films at larger distance from the target may be due to their elemental composition (film: H – 56.8%, Li – 0.6%, O – 13.3%, and Al – 1.6% and OSLD: Al – 52.9% and O – 47.1%) which were made with less atomic number materials. The OSLDs are made up of high-density material that can respond better than films which were made with elemental composition of less atomic number. As reported in the literature, OSLD is not energy dependent for 6–18 MV photons energies.[20] However, the response of the OSLD may be more with scattered radiation from collimator and phantom in the out of field. The over-response of OSLD may be due to relatively high-energy dependency nature of OSLD compared to film.

Furthermore, for the OARs located at larger distances, the scatter radiation is predominant with less energy, because of which the OSLD materials make a perfect match for photoelectric interaction. The interaction makes the OSLD more sensitive to detect the radiation dose in far of field OARs. The observation of film response with far of distances may also be due to experimental limitations such as the size of the film where it is been cut to a very small dimension in such a way that the spindles could have been altered, probable damage during placement of films, and the placement of film parallel to the beam which are prone to be influenced with directional dependency.[21] All these combined issues make the film less sensitive/large difference from TPS for low-dose levels.

Duhaini *et al*.[22] conducted a study to measure the dose received by the treated breast as well as the dose to the lungs in cancer patients undergoing breast radiotherapy and estimate the probability of radiation-induced cancer in a 3DCRT treatment planning technique. The measured doses were compared with those calculated by the TPS. The difference between the measured surface skin dose of the breast and the TPS

Table 5: Lifetime attributable risk values of left lung, right lung, and right breast

	Left lung	Right lung	Right breast
3DCRT	1.73±2.01	0.73±1.21	0.33±1.65
IMRT_C_FF	1.92±0.45	0.91±0.23	0.99±0.13
IMRT_T_FF	1.57±0.27	0.89±0.17	1.09±2.14
VMAT_C_FF	2.82±1.09	1.82±1.32	2.12±2.02
VMAT_T_FF	2.22±0.20	2.05±0.79	2.35±0.29
IMRT_C_FFF	1.90±0.98	0.99±1.08	0.89±0.58
IMRT_T_FFF	1.42±0.23	0.88±0.20	0.95±1.45
VMAT_C_FFF	2.92±0.14	2.23±2.14	2.69±1.75
VMAT_T_FFF	2.32±1.04	2.02±1.64	1.92±1.40
HYB 80/20	2.38±0.56	1.98±1.50	1.55±0.50
HYB 70/30	2.13±1.02	1.93±1.62	1.23±0.17
*P**		0.01	

*Calculated from Student's *t*-test LAR values are expressed per 100 persons. Assuming age at exposure of 30 years. LAR: Lifetime attributable risk, 3DCRT: 3D conformal radiotherapy, IMRT: Intensity-modulated radiation therapy, VMAT: Volumetric modulated arc therapy, HYB: Hybrid, FF: Flattening filter, FFF: FF free

calculated was <5%. As far as ipsilateral lungs are concerned, there is a difference of 10% in the superior medial and 14.3% in the superior lateral lungs. With the contralateral lungs, there is a difference of 17.7% in the superior medial and 24.6% in the superior lateral lungs. In the present study, the target dose differences with both OSLD and films were within 5% in agreement with TPS-calculated values and the peripheral OAR doses ranged between 5% and 15% comparing with all the treatment techniques.

Sánchez-Nieto *et al.*[23] stated that technology advancements such as IMRT and VMAT were liable for an increase in doses received to out-of-field OARs. Fortunately, such a dose increase at a distance is greatly compensated by a significant reduction in the areas getting high doses. Even if new technologies were not thought to cause more secondary radiation-induced cancers than conventional techniques, a continuous effort should be made to reduce the far-of-field doses delivered to patients as a continued radiotherapy improvement strategy, thus adhering to previous International Commission on Radiation Protection (ICRP) recommendations regarding optimization.[24]

The risk of second primary cancer is very important on pediatric cancer patients, but the incidence of second primary cancers has been rising steadily, largely due to improving survival rates from cancer. From 1975 to 1979, 9% of all cancers represented a second primary cancer. That number has increased such that 19% of cancers diagnosed between 2005 and 2009 were a second primary cancer. Furthermore, there are reports that the number of women developing lung tumors following breast cancer is constantly growing. Approximately 47% of relapses in women treated for breast cancer had metastases, and 40% were second primary lung tumors.[25]

Several studies have been conducted to calculate the secondary cancer risks for patients receiving radiotherapy. In the current study, we analyzed actual secondary cancer risks in terms of LAR for specific organs such as left lung, right lung, and right breast which had higher EAR values to aid appropriate treatment strategy by radiation oncology team. Apart from these three OARs, the thyroid EAR values were also noticed with relatively higher risk, which also needs attention while finalizing the treatment plan. Reportedly, survivors are at 10%–50% higher risk of developing nonbreast secondary cancers than members of the general population. Although advanced treatment techniques are successful in reducing toxicities associated with high exposure doses, they sometimes necessitate more Monitor Units (MUs) than conventional tangential techniques which is of greater concern.

Conclusion

Dose measurements in 23 distinct locations, including both PTV and OARs, were successfully done using OSLDs and EBT3 films with Rando phantom for 11 different treatment approaches. Though the readings acquired by both methods are within 5% of the target and 15% of the OARs. Our results reveal that both films and OSLDs are effective for in-phantom dose measurements of adjacent OARs; however, OSLDs were found to be superior in assessing OAR doses at larger distances from the target. The Secondary Cancer Risk (SCR) of the thyroid and right breast, according to our findings, indicates that it cannot be disregarded during decision-making process. Considering the secondary cancer risk associated with the patients treated in the younger age group, it is suggested that *in vivo* dose estimation should be a part of treatment quality audit whenever possible.

Financial support and sponsorship

Nil.

Conflicts of interest

There are no conflicts of interest.

References

1. van der Giessen PH. Peridose, a software program to calculate the dose outside the primary beam in radiation therapy. Radiother Oncol 2001;58:209-13.
2. Grantzau T, Mellemkjær L, Overgaard J. Second primary cancers after adjuvant radiotherapy in early breast cancer patients: A national population based study under the Danish Breast Cancer Cooperative Group (DBCG). Radiother Oncol 2013;106:42-9.
3. Berrington de Gonzalez A, Curtis RE, Gilbert E, Berg CD, Smith SA, Stovall M, *et al.* Second solid cancers after radiotherapy for breast cancer in SEER cancer registries. Br J Cancer 2010;102:220-6.
4. Lee B, Lee S, Sung J, Yoon M. Radiotherapy-induced secondary cancer risk for breast cancer: 3D conformal therapy versus IMRT versus VMAT. J Radiol Prot 2014;34:325-31.
5. Hall EJ, Wuu CS. Radiation-induced second cancers: The impact of 3D-CRT and IMRT. Int J Radiat Oncol Biol Phys 2003;56:83-8.
6. Olaciregui-Ruiz I, Beddar S, Greer P, Jornet N, McCurdy B, Paiva-Fonseca G, *et al. In vivo* dosimetry in external beam photon radiotherapy: Requirements and future directions for research, development, and clinical practice. Phys Imaging Radiat Oncol 2020;15:108-16.
7. La Tessa C, Berger T, Kaderka R, Schardt D, Körner C, Ramm U, *et al.* Out-of-field dose studies with an anthropomorphic phantom:

Comparison of X-rays and particle therapy treatments. Radiother Oncol 2012;105:133-8.
8. Kaderka R, Schardt D, Durante M, Berger T, Ramm U, Licher J, *et al.* Out-of-field dose measurements in a water phantom using different radiotherapy modalities. Phys Med Biol 2012;57:5059-74.
9. Zhang D, Li X, Gao Y, Xu XG, Liu B. A method to acquire CT organ dose map using OSL dosimeters and ATOM anthropomorphic phantoms. Med Phys 2013;40:081918.
10. Van den Heuvel F, Defraene G, Crijns W, Bogaerts R. Out-of-field contributions for IMRT and volumetric modulated arc therapy measured using Gafchromic films and compared to calculations using a superposition/convolution based treatment planning system. Radiother Oncol 2012;105:127-32.
11. Athar BS, Paganetti H. Comparison of second cancer risk due to out-of-field doses from 6-MV IMRT and proton therapy based on 6 pediatric patient treatment plans. Radiother Oncol 2011;98:87-92.
12. Yukihara EG, Yoshimura EM, Lindstrom TD, Ahmad S, Taylor KK, Mardirossian G. High-precision dosimetry for radiotherapy using the optically stimulated luminescence technique and thin Al2O3: C dosimeters. Phys Med Biol 2005;50:5619-28.
13. Aznar MC, Andersen CE, Bøtter-Jensen L, Bäck SA, Mattsson S, Kjaer-Kristoffersen F, *et al.* Real-time optical-fibre luminescence dosimetry for radiotherapy: Physical characteristics and applications in photon beams. Phys Med Biol 2004;49:1655-69.
14. Andersen CE, Marckmann CJ, Aznar MC, Bøtter-Jensen L, Kjaer-Kristoffersen F, Medin J. An algorithm for real-time dosimetry in intensity-modulated radiation therapy using the radioluminescence signal from Al2O3: C. Radiat Prot Dosimetry 2006;120:7-13.
15. Jursinic PA. Characterization of optically stimulated luminescent dosimeters, OSLDs, for clinical dosimetric measurements. Med Phys 2007;34:4594-604.
16. Kry SF, Salehpour M, Followill DS, Stovall M, Kuban DA, White RA, *et al.* The calculated risk of fatal secondary malignancies from intensity-modulated radiation therapy. Int J Radiat Oncol Biol Phys 2005;62:1195-203.
17. Howell RM, Scarboro SB, Kry SF, Yaldo DZ. Accuracy of out-of-field dose calculations by a commercial treatment planning system. Phys Med Biol 2010;55:6999-7008.
18. Kry SF, Titt U, Pönisch F, Followill D, Vassiliev ON, White RA, *et al.* A monte carlo model for calculating out-of-field dose from a varian 6 MV beam. Med Phys 2006;33:4405-13.
19. Siegel JA, Greenspan BS, Maurer AH, Taylor AT, Phillips WT, Van Nostrand D, *et al.* The BEIR VII estimates of low-dose radiation health risks are based on faulty assumptions and data analyses: A call for reassessment. J Nucl Med 2018;59:1017-9.
20. Ponmalar R, Manickam R, Ganesh KM, Saminathan S, Raman A, Godson HF. Dosimetric characterization of optically stimulated luminescence dosimeter with therapeutic photon beams for use in clinical radiotherapy measurements. J Cancer Res Ther 2017;13:304-12.
21. Suchowerska N, Hoban P, Butson M, Davison A, Metcalfe P. Directional dependence in film dosimetry: Radiographic and radiochromic film. Phys Med Biol 2001;46:1391-7.
22. Duhaini I, Hodroj N, Farhat F, Ayoubi S, Maarouf A, Korek M. Organ at risk dose measurements following radiotherapy treatment for breast cancer patients. Health Technol. 2018;8:405-10.
23. Sánchez-Nieto B, Romero-Expósito M, Terrón JA, Irazola L, Paiusco M, Cagni E, *et al.* Intensity-modulated radiation therapy and volumetric modulated arc therapy versus conventional conformal techniques at high energy: Dose assessment and impact on second primary cancer in the out-of-field region. Rep Pract Oncol Radiother 2018;23:251-9.
24. Moding EJ, Kastan MB, Kirsch DG. Strategies for optimizing the response of cancer and normal tissues to radiation. Nat Rev Drug Discov 2013;12:526-42.
25. Mariotto AB, Rowland JH, Ries LA, Scoppa S, Feuer EJ. Multiple cancer prevalence: A growing challenge in long-term survivorship. Cancer Epidemiol Biomarkers Prev 2007;16:566-71.